PHYSICAL REVIEW A VOLUME 59, NUMBER 4 APRIL 1999

Efficient phase conjugation via two-photon coherence in an optically dense crystal

B. S. Ham,[1] P. R. Hemmer,[2] and M. S. Shahriar[1]
[1]*Research Laboratory of Electronics, Massachusetts Institute of Technology, Cambridge, Massachusetts 02139*
[2]*U.S. Air Force Research Laboratory, Hanscom Air Force Base, Massachusetts 01731*
(Received 25 November 1998)

We demonstrate efficient phase conjugation in an inhomogeneously broadened rare-earth doped crystal using electromagnetically induced transparency. The observed frequency conversion efficiency of the phase conjugate in energy over a backward pump beam is as high as 10% with ~1/4 of maximal Raman coherence. This efficient phase conjugation has potential applications of nonlinear optical processes such as frequency up-conversion and Raman excited spin-echo optical memory. [S1050-2947(99)50704-X]

PACS number(s): 42.65.Hw, 42.50.Gy, 42.70.Mp, 42.79.Nv

Recent observation of electromagnetically induced transparency [1] (EIT) in solid crystals [2] presents potential applications of EIT using solids for nonlinear optical processes, such as inversionless lasers [3], high-density optical memory [4], and enhanced four-wave mixing [5]. For these applications, large coherence amplitude is desired. For example, efficient up-conversion using EIT was initially proposed for atomic systems [6] and experimentally demonstrated (using atomic gas or vapors) for sum-frequency generation [7], enhanced four-wave mixing [8], and gain of phase conjugation [9]. Recently Jain *et al.* observed efficient frequency conversion using high-power pulsed lasers in Pb vapor [10]. In that experiment, they observed frequency conversion efficiency (in power) as high as 40% with near maximal Raman coherence. In four-wave-mixing experiments high-gain phase conjugation (the power ratio of the phase conjugate to input signal) was observed using a low-power input signal with EIT or coherent population trapping [11], but the conversion efficiency (the power ratio of the phase conjugate to the backward pump) was less than ~1% [9,12].

In this paper, we demonstrate efficient phase conjugation in a solid material using EIT. Previously we demonstrated that four-wave-mixing generation could be enhanced by EIT using Pr^{3+}-doped Y_2SiO_5 (Pr:YSO) [5]. In that experiment, all laser beams were cw and forward propagating. In the present experiment, we have used a phase-conjugate scheme with pulsed lasers and achieved more than 100 times better conversion efficiency. Aside from enhanced efficiency, the use of a phase-conjugate scheme with pulsed lasers is more suitable for applications to optical memory, turbulence diagnostics, and novelty filters. Significantly, we have achieved this high conversion efficiency with an unstabilized laser (frequency jitter ~80 MHz), even though atomic vapor studies show that the laser jitter should degrade the Raman coherence in an inhomogeneously broadened system [13]. We attribute this higher conversion efficiency to suppressed spectral hole-burning when the laser jitter exceeds the hyperfine splitting in the ground state of Pr:YSO. Finally, we have numerically analyzed the experimental data. From the analysis, we have deduced that the observed efficiency corresponds to ~1/4 of maximal Raman coherence.

The physics of the enhanced nonlinear optical processes owing to EIT is based on the quantity $|\chi_D^{(3)}/\mathrm{Im}\chi_D^{(1)}|^2$, where the third-order nonlinear susceptibility $\chi_D^{(3)}$ is enhanced, while first-order linear susceptibility $\mathrm{Im}(\chi_D^{(1)})$ is suppressed at line center [6]. In a three-level Λ-type system, as seen in Fig. 1, the laser fields F and S provide Raman coherence on the transition $|a\rangle \leftrightarrow |b\rangle$. The strength of the Raman coherence ρ_{ab} is proportional to the product of the applied Rabi frequencies: $\rho_{ab} \propto \Omega_S \Omega_F$, where Ω_S and Ω_F are Rabi frequencies of the S and F fields, respectively. Here it should be noted that the Rabi frequency should be larger than the inhomogeneous width or dephasing rate of the transition $|a\rangle \leftrightarrow |b\rangle$. The phase-conjugate intensity I_C is proportional to the product of the square of the coherence ρ_{ab} and backward pump intensity I_B: $I_C \propto [\mathrm{Re}(\rho_{ab})]^2 I_B$. Therefore the phase-conjugate intensity I_C increases continuously until saturated as the Raman laser intensities increase. This fact was experimentally demonstrated using Pb [10] (pulse) and Rb [12] (cw) vapors. With maximal Raman coherence, the frequency conversion efficiency can reach up to ~140% [10].

For the current study of phase conjugation in solids, we used 0.05 at. % Pr^{3+}-doped Y_2SiO_5, in which Pr^{3+} ions substitute for Y^{3+} ions. In Fig. 1, the optical transitions ($|a\rangle \leftrightarrow |c\rangle$ and $|b\rangle \leftrightarrow |c\rangle$) belong to the $^3H_4 \leftrightarrow {}^1D_2$ manifold, which has a resonance frequency of ~606 nm. Each ground and excited level has three hyperfine states [14]. The optical

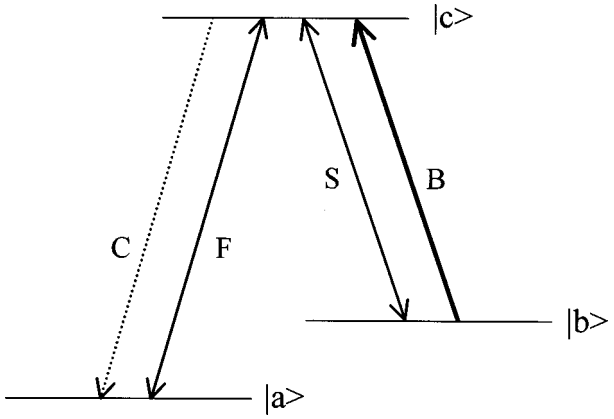

FIG. 1. Energy-level diagram for phase conjugation owing to Raman coherence ρ_{ab}. The Raman coherence ρ_{ab} is prepared by the laser beam F and S. $|a\rangle$, $|b\rangle$, and $|c\rangle$ denote energy states $\pm 3/2$ ($^3H_4$), $\pm 1/2$ ($^3H_4$), and $\pm 1/2$ ($^1D_2$), respectively, in Pr:YSO.

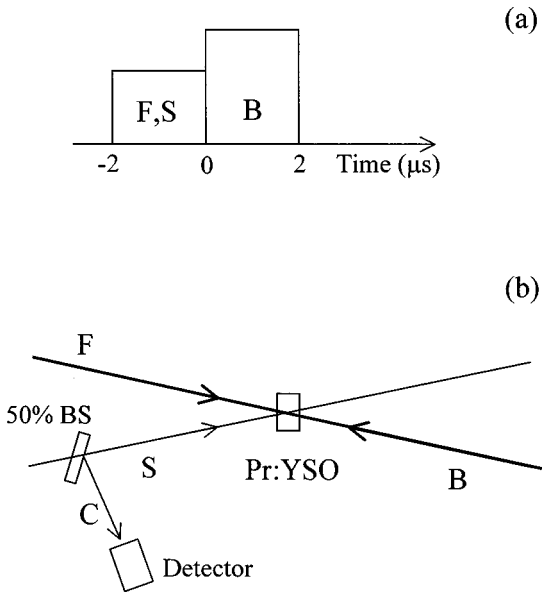

FIG. 2. (a) Pulse sequence and (b) a schematic of the experimental setup.

inhomogeneous width for the transitions is ~4 GHz at liquid-helium temperatures, which is much wider than the hyperfine splittings. The frequency difference between the state $|a\rangle$ and the state $|b\rangle$ is 10.2 MHz [15]. Due to the large optical inhomogeneous broadening, each Pr ion has one of the nine transitions: the selection rule breaks down because of low site symmetry [14]. The optical homogeneous dephasing rate is linearly proportional to the excitation laser intensity [15]. The extrapolation to zero excitation intensity at 1.4 K yields 2.4 kHz of optical homogeneous width and increases 1 kHz per every intensity increase of 4 W cm^2 [15]. Due to the phonon interactions, the optical homogeneous linewidth is also widened as temperature increases. We observed that the optical homogeneous width increases exponentially as temperature increases from 4 K to 6 K in Pr:YSO, while the spin homogeneous width is almost constant [4]. The optical depopulation decay time is 164 μs at 1.4 K [15]. Due to the long population decay time on the ground-state hyperfine levels (~100 s at 6 K) [14], optical spectral hole-burning persists until the populations are redistributed among the three hyperfine levels. We measured inhomogeneous width for the transition $|a\rangle \leftrightarrow |b\rangle$ to be 29 kHz using rf-optical double resonance [16]. Pr:YSO is optically thick, and the measured absorption coefficient is $\alpha = 10\ \text{cm}^{-1}$ (when there is no spectral hole-burning) [15].

The experimental setup for phase conjugation is shown in Fig. 2. The laser pulses *F* and *S* are simultaneously forward propagating with a small angle of 80 mrad. These pulses excite the Raman coherence between the levels $|a\rangle$ and $|b\rangle$. The probe pulse *B* is aligned to be counterpropagating to the *F*, and follows at the end of the *F* and *S*. To satisfy the phase-matching condition $\mathbf{k}_C = \mathbf{k}_F + \mathbf{k}_B - \mathbf{k}_S$, the phase-conjugate signal travels opposite to the signal *S*. To detect the phase-conjugate signal, we put a 50% beam splitter in the path of the *S*. All the laser pulses *F*, *S*, and *B* are from a ring dye laser (Coherent Model 699) pumped by a Spectra Physics argon-ion laser. To provide the three different laser frequencies, acousto-optic modulators are used. All three laser

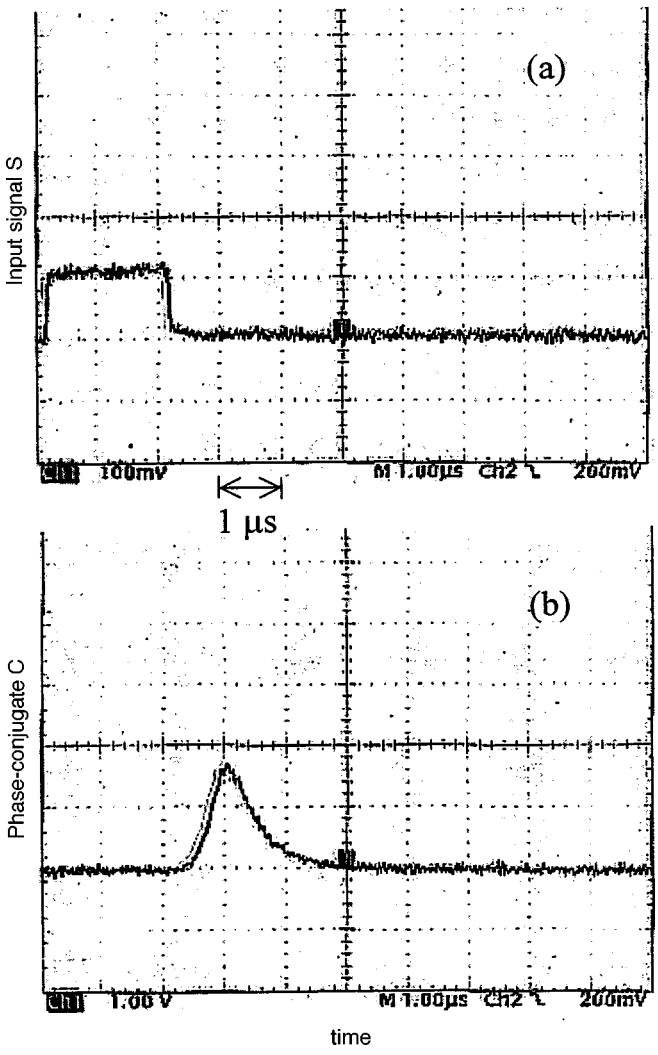

FIG. 3. (a) Input signal *S* with attenuation by ND 2.0 and (b) phase conjugate *C* without attenuation.

frequencies have a relative frequency jitter of less than 1 kHz. The laser beams are focused into the sample by a 30-cm focal-length lens. The beam diameters ($1/e$ in intensity) are ~100 μm in the crystal. The applied cw laser powers of *F*, *S*, and *B* are 6, 4, and 26 mW, respectively. The laser intensity jitter is ~10%. To generate pulses, we used rf switches driven by a digital pulse generator. The phase-conjugate signal is detected by a fast photodiode directly connected to a fast oscilloscope (Tektronix TDS 640A; 5 Gsample/s). The sample Pr:YSO is in a cryostat and the temperature is kept at 5 K. The sample dimension is $3\times3.5\times4\ \text{mm}^3$ and its optical axis is along the 3-mm direction. The laser beams are almost parallel to the optical *b* axis. We used linearly polarized laser beams for the experiments.

Figures 3(a) and 3(b) show the input signal *S* and phase conjugate *C* for individual pulses with no averaging on the oscilloscope, respectively. Because of the broad laser bandwidth (80 MHz) and the slow pulse repetition rate of 20 Hz ($\gamma_{\text{spin}} = 0.5$ ms), the individual Raman coherence does not accumulate. For the data in Fig. 3(a), the input signal *S* is attenuated with a neutral density filter (ND 2.0). Its corrected peak voltage on the oscilloscope is therefore 10 V. The peak voltage of the backward pump *B* is 65 V (not shown). The

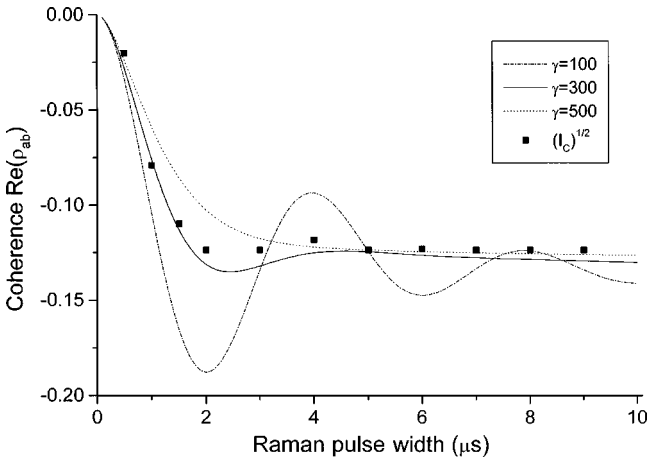

FIG. 4. Numerical simulation of the Raman induced coherence $\mathrm{Re}(\rho_{ab})$: $\Omega_F=200$, $\Omega_S=160$, $\Gamma_{\mathrm{opt}}=2$, $\gamma_{\mathrm{spin}}=0.5$, $\Gamma_{\mathrm{spin}}=0$, and $\Delta_{\mathrm{inh}}(|a\rangle\leftrightarrow|b\rangle)=25$ kHz. γ is an optical coherence decay rate (kHz).

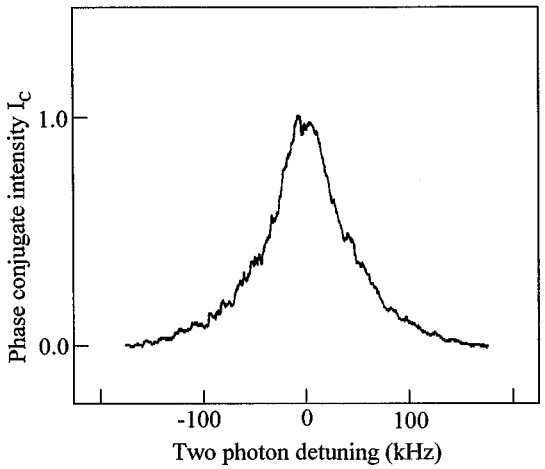

FIG. 5. Phase-conjugate intensity I_C versus two-photon detuning.

voltage of the phase-conjugate intensity I_C in Fig. 3(b), however, experiences a 50% cut in intensity due to the beam splitter (see Fig. 2). Therefore, the peak power and energy ratio of the phase conjugate C to the probe B is 4.9% and 2.3%, respectively. However, the measured conversion efficiencies must be corrected due to the limited spatial overlap and through optical density. Applying an estimated correction factor of $\exp(-1.5)$ gives frequency conversion efficiencies of $\sim$22% in peak power and $\sim$10% in energy.

To study how the phase conjugation depends on Raman pulse area, we varied the Raman pulse width, always keeping the probe (fixed at 2-μs pulse width) at the end of the Raman pulse. As the Raman pulse width was shortened below 2 μs, we found that the phase-conjugate intensity I_C decreased roughly linearly. For the Raman pulses longer than 2 μs, the I_C was almost constant. The results appear in Fig. 4 with square marks. To analyze these data, we solved time-dependent density-matrix equations and plotted the Raman-induced coherence $\mathrm{Re}(\rho_{ab})$ as a function of the Raman pulse width. The numerical plots are for three different cases of the optical dephasing rate γ: $\gamma\ll\Omega$, $\gamma\sim\Omega$, and $\gamma\gg\Omega$, where $\Omega_2=\Omega_S^2+\Omega_F^2$. When the Raman Rabi frequency Ω is larger than the optical dephasing rate γ (dash-dot curve), the coherence $\mathrm{Re}(\rho_{ab})$ oscillates with a period of 2π. This oscillation is explained as Rabi flopping between a bright state $|+\rangle$ (nontrapped superposition state of levels $|a\rangle$ and $|b\rangle$) and the excited state $|c\rangle$: $|+\rangle=(\Omega_S|a\rangle+\Omega_F|b\rangle)/\Omega$ [17]. When the Rabi frequency is smaller than the optical dephasing rate γ (dotted curve), the oscillation quickly damps out. For the numerical simulations, we assumed a closed three-level system and used the experimental parameters. For the Rabi frequencies of the F and S we did not measure them experimentally, but guessed best values through EIT experiments and the numerical simulations.

For the best-fit curve of the experimental data, we choose a reference with a data point at 5-μs Raman pulse width, and plotted the square root of the data. The reason for the square root is because the phase-conjugate intensity is proportional to the square of the Raman coherence. As we see in Fig. 4, the experimental data nearly fit into the theoretical curve for $\gamma=300$ kHz. From those plots, we conclude that the Raman coherence is saturated at $\sim$2 μs (π-pulsed area), and the experimental values of γ should be larger than the Raman Rabi frequency Ω. We also deduce that the Raman pulse in the experiment [Fig. 3(b)] induces $\sim$1/4 of the maximal coherence (-0.5) of ρ_{ab}.

Figure 5 shows phase-conjugate intensity I_C versus two-photon detuning. For the two-photon detuning, we simply scan the frequency of the input signal S through the resonance. The width [full width at half maximum (FWHM)] of the phase-conjugate signal (30 sample average) is $\sim$95 kHz, which is power broadened but much narrower than the effective optical dephasing rate γ (or laser jitter). This demonstrates that the phase conjugation is enhanced by EIT. The width of the phase conjugate C should decrease at least down to the spin inhomogeneous width as the Raman pulse intensity decreases.

In summary, we demonstrated efficient phase conjugation based on electromagnetically induced transparency in an optically dense solid medium using weak power lasers. The observed frequency conversion efficiency of the phase conjugation is $\sim$10% in energy with $\sim$1/4 of maximal coherence. Such efficient phase conjugation is useful for nonlinear optical applications such as the Raman echo optical memory, frequency up-conversion, inversionless lasers, and turbulence diagnostics.

We acknowledge helpful discussions with Professor S. Ezekiel of the Massachusetts Institute of Technology. This research was supported by the U.S. Air Force Research Laboratory (Grant No. F30602-96-2-0100) and the U.S. Air Force Office of Scientific Research (Grant No. F49620-96-1-0395).

[1] S. E. Harris, Phys. Today **50** (7), 36 (1997), and references therein.

[2] Y. Zhao, C. Wu, B. S. Ham, M. K. Kim, and E. Awad, Phys. Rev. Lett. **79**, 641 (1997); B. S. Ham, M. S. Shahriar, and P. R. Hemmer, Opt. Commun. **144**, 227 (1997), and references therein.

[3] A. S. Zibrov, M. D. Lukin, D. E. Nikonov, L. Hollberg, M. O. Scully, V. L. Velichansky, and H. G. Robinson, Phys. Rev. Lett. **75**, 1499 (1995).

[4] B. S. Ham, M. S. Shahriar, M. K. Kim, and P. R. Hemmer, Opt. Lett. **22**, 1849 (1997).

[5] B. S. Ham, M. S. Shahriar, and P. R. Hemmer, Opt. Lett. **22**, 1138 (1997), and references therein.

[6] S. E. Harris, J. E. Field, and A. Imamoglu, Phys. Rev. Lett. **64**, 1107 (1990).

[7] K. Hakuta, L. Marmet, and B. P. Stoicheff, Phys. Rev. Lett. **66**, 596 (1991); G. Z. Zhang, K. Hakuta, and B. P. Stoicheff, *ibid*. **71**, 3099 (1993).

[8] M. Jain, G. Y. Yin, J. E. Field, and S. E. Harris, Opt. Lett. **18**, 98 (1993); Y. Q. Li and M. Xiao, *ibid*. **21**, 1064 (1996).

[9] P. R. Hemmer, D. P. Katz, J. Donoghue, M. Cronin-Golomb, M. S. Shahriar, and P. Kumer, Opt. Lett. **20**, 982 (1995).

[10] M. Jain, H. Xia, G. Y. Yin, A. J. Merriam, and S. E. Harris, Phys. Rev. Lett. **77**, 4326 (1996).

[11] G. Alzetta, A. Gozzini, L. Moi, and G. Orriols, Nuovo Cimento B **36**, 5 (1976); H. R. Gray, R. M. Whitley, and C. R. Stroud, Jr., Opt. Lett. **3**, 218 (1978).

[12] B. Lu, W. H. Burkett, and M. Xiao, Opt. Lett. **23**, 804 (1998); T. T. Grove, M. S. Shahriar, P. R. Hemmer, P. Kumar, V. S. Sudarshanam, and M. Cronin-Golomb, *ibid*. **22**, 769 (1997).

[13] Y.-Q. Li and M. Xiao, Phys. Rev. A **51**, 4959 (1995).

[14] K. Holliday, M. Croci, E. Vauthey, and U. P. Wild, Phys. Rev. B **47**, 14 741 (1993).

[15] R. W. Equall, R. L. Cone, and R. M. Macfarlane, Phys. Rev. B **52**, 3963 (1995).

[16] L. E. Erickson, Opt. Commun. **21**, 147 (1977).

[17] B. S. Ham, M. S. Shahriar, M. K. Kim, and P. R. Hemmer, Phys. Rev. B **58**, R11 825 (1998).